Latin American Journal of Solids and Structures
www.lajss.org

Effect of an Opening on Reinforced Concrete Hollow Beam Web Under Torsional, Flexural, and Cyclic Loadings

Abstract

Hollow sections have been increasingly applied in the construction of buildings, bridges, offshore structures, and towers for passing electrical and mechanical pipes or other utilities. Torsion caused by external force is a weakness of hollow sections that is rarely investigated. In particular, the behavior of hollow sections with high-strength concrete (HSC) and ultra-high performance concrete (UHPC) remains poorly studied. This study aims to examine the behavior of a reinforced concrete hollow beam with opening and compare it with a hollow beam without opening. The hollow beam with an opening is modeled using the finite element method and analyzed under torsional, flexural, and cyclic loading with HSC and UHPC materials. The effect of the opening section size on the behavior of hollow beam is also evaluated. The openings created in the web of hollow beams led to a decrease in beam capacity although the hollow beam with small opening can carry almost the same load as that of hollow beam without an opening. The result also shows that the capacity of UHPC beams for twisting is twice that of HSC beams.

Keywords

Cyclic load, Flexural load, Finite element, Hollow beam, High-strength concrete (HSC), Torsion load, Ultrahigh-performance concrete (UHPC)

Sarah Jabbar [a,d]
Farzad Hejazi [b]
H. Mahir Mahmod [c,d]

[a] University Putra Malaysia, Malaysia, Email: sarahsaleem2015@gmail.com.
[a] Ministry of municipalities, Iraq
[b] Corresponding author: University Putra Malaysia, Malaysia. Email: farzad@fhejazi.com, Tel: (+6)014-2221092
[c] University Putra Malaysia, Malaysia. Email:mahir.mahmod@gmail.com
[d] Ministry of Science and Technology, Iraq, Email: mahir.mahmod@gmail.com

http://dx.doi.org/10.1590/1679-78252629

Received 18.11.2015
In revised form 29.03.2016
Accepted 03.04.2016
Available online 12.04.2016

1 INTRODUCTION

High-strength concrete (HSC) and ultra-high performance concrete (UHPC) have recently been used in new structures. HSC involves higher production costs compared with normal-strength concrete (NSC), but it is applied in constructing various building structures, particularly in bridges, because of its advantages (Lopes and Bernardo, 2009). UHPC is a special type of concrete that has attracted interest from many civil engineers because of its extraordinary potential in terms of strength and durability performance. The most up-to-date knowledge and technology of concrete manufacturing are implemented in the production and application of UHPC (Chen and Graybeal, 2011).

In 2015, Yoo and Yoon studied the structural performance of UHPC beams with different steel fibers. Their results indicated that steel fibers significantly improve the load carrying capacity, post-cracking stiffness, and cracking response, but decrease ductility. Specifically, with the inclusion of 2% volume of steel fibers, approximately 27%–54% higher load carrying capacity and 13%–73% lower ductility are obtained. In addition, an increase in the length of smooth steel fibers and the use of twisted steel fibers enhance the post-peak response and ductility; however, no noticeable difference is found in the load carrying capacity and post-cracking stiffness. Cracking response is in accordance with fiber length and type (Yoo and Yoon, 2015).

Owing to the high-strength characteristics of HSC and UHPC sections, these materials are applied in hollow beam sections. The hollow sections exhibit desirable strength against bending moments but possess poor tensional loads. In real building structures, reinforced concrete beams are subjected to torsion as a result of external load outside of the shear center of the cross-section or deformations resulting from the continuity of beams. Torsion was considered to be a secondary effect for a certain period; it was not explicitly regarded in design, and its influence was part of the overall factor of safety, which is not an economical design (Namiq, 2008).

Lopes and Bernardo (2009) found that beams with high-strength concrete under torsion have four different types of fault that rely on reinforcements. From the lowest to the highest ratios of reinforcement, failures of beams include brittle fracture caused by insufficient reinforcement, fragile fracture caused by corner cracking, crisp failure caused by insufficient strength of the concrete, and ductile failure. The failure becomes more fulminatory when the concrete strength of beam is increased. In 2013, they conducted a plastic analysis and evaluated the twist capacity of high-strength concrete hollow beams under pure torsion. They reported that an increase in the compressive strength of the concrete leads to a small decrease in plastic twist capacity (Bernardo and Lopes, 2013). In 2014, they investigated the cracking and defeat modes in hollow beams under torsion using HSC. The result indicated that the use of HSC leads to less ductile and cracked beams compared with NSC and that crack is more fragile and noisier (Lopes and Bernardo, 2014). Hii and Al-Mahaidi (2006) investigated experimental and numerical realization on the torsional strengthening of solid and hollow RC beams externally bonded with carbon fiber-reinforced polymer that boosts both cracking and ultimate strengths up to 40% and 78%, respectively(Hii and Al-Mahaidi, 2006).

Rather than hollow beams, the RC sections with web openings are also frequently used in construction for passing electrical and mechanical utilities as shown in Figure 1. Flexure is considered an important parameter for structural design service load (Patel et al., 2014).

Hafiz et al. (2014) evaluated the effects of openings on the behavior of reinforced concrete beams without special reinforcement on the opening zone. The reinforced concrete rectangular beams with circular openings of diameter less than 44% of the depth of beam (D) exerted no effect on the ultimate load capacity; however, circular openings with a diameter greater than 44% of D reduced the ultimate load capacity by at least 34.29%. Their team also realized that the circular opening exhibits more strength than the tantamount square opening, with a variation of 9.58% in ultimate load (Hafiz et al., 2014).

Most beams in recent structures are designed for different types of loads, such as dynamic load caused by earthquake excitation, vehicle and train vibration, rotary machines, and any similar source of vibration. The failure mechanism of the beam subjected to the dynamic load is more complex than that of the beam imposed to static loads; therefore, evaluating failure pattern of the beam under dynamic loads at ultimate loading conditions is vital. Most of the practical problems of structural dynamics analysis are resolved using numerical methods (Torii and Machado, 2012).

Inoue and Egawa (1996) examined the flexural and shear behavior of hollow beam under cyclic load. Their result indicated that the ultimate deformation and energy dissipation capacity of the hollow beam are smaller than those of the solid beam and that the ultimate failure is more brittle. In addition, the diagonal crack can be generated in the early stages, leading to a considerable increase in the strain of stirrups(Inoue and Egawa, 1996).

The implementation of incremental plasticity for multiaxial cyclic loading in FEM analysis is a challenging issue in the convergence of iteration and entails a heavy computational process that is time-consuming (Li et al., 2006). Guleria (2014) discussed the seismic performance of solid and hollow reinforced concrete beams in framed buildings. Their results showed that the hollow members help reduce forces without failure, achieving an economical building design. Using hollow sections also reduces the overturning moment and concrete usage (Guleria, 2014).

Figure 1: Beams with openings.

Creating an opening in the solid beam decreases shear resistance, and the opening is required to increase the number of stirrups especially under flexural and cyclic load. The behavior of HSC and UHPC hollow beams with openings has not been completely examined. Therefore, this study evaluated the effect of an opening on the hollow beam with HSC and UHPC materials with half stirrups above and under the opening subjected to torsional, flexural, and cyclic load. A parametric study was also conducted to determine the effect of the web opening size on hollow beams.

2 HOLLOW BEAM WITH A WEB OPENING

Structural hollow sections have been increasingly used. These hollow sections are used for passing electrical and mechanical utilities, as well as reducing story height and material and construction costs. Non-prismatic beams (hollow beams) could be appropriately used as ground beams in residential buildings. Furthermore, the use of non-prismatic beams allows other beams to cross one another without the need for relocating these pipes. The presence of web openings in a reinforced concrete beam reduces the capacity of the beam to carry load and increases its service-load deflections and crack widths. In this study, these effects are evaluated by numerical modeling of a hollow beam. For this purpose, the hollow beam examined by Lopes et al. (2009) was considered, and the effect of a hollow section opening on the capacity of the beam is evaluated. The details of the beam under consideration are presented in the following section.

2.1 Geometric Beam

A hollow beam with a (600*600) mm section size is used as presented in the study of Lopes et al. (2009) (Figure 2). The beam is considered a benchmark to evaluate the effect of an opening on the behavior of a beam subjected to loads. The maximum capacity of the beam under torsion is about 254.8 KN.m based on the study by Lopes et al.

This parametric study was conducted to investigate the effect of the opening size on the capacity of the beam. Five beams were modeled; all the beams had a clear span (Lc), depth (d), and width (b) of 6000, 600, and 600 mm, respectively. Figure 2 shows the geometry and dimensions of the beams, and Figure 3 shows the modeled beams.

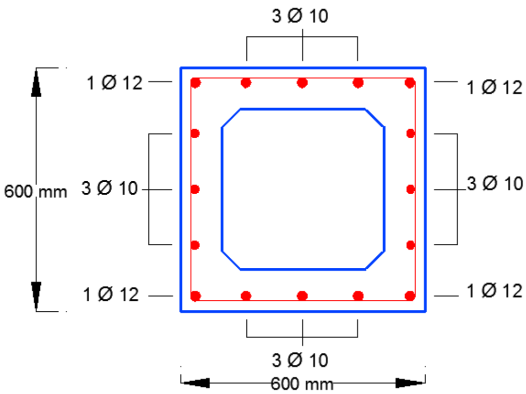

(a) Cross-section (mm).

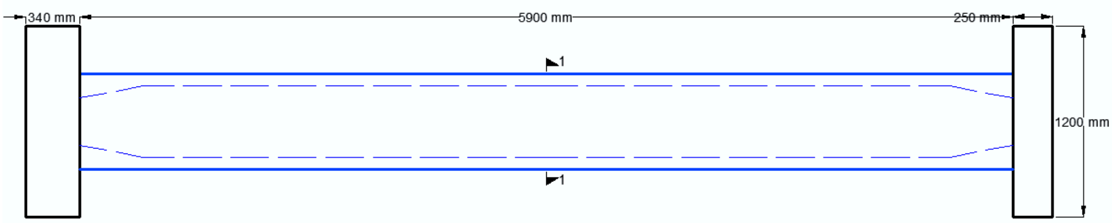

(b) Longitudinal view (mm).

Figure 2: Reinforced concrete beam(Lopes and Bernardo, 2009).

As shown in Figure 3, five different sections of the beam were considered: the solid section (S), hollow beam (H), and hollow beam with square openings that measure 100 mm (H_{100}), 200 mm (H_{200}), and 300 mm (H_{300},), as listed in Table 1. The center-to center distance of the opening was 500 mm for all models. 3D tetrahedral element is used to model the beam in this study because the solid (or continuum) elements in ABAQUS can be used for linear analysis and for complex nonlinear analyses that involve with contact, plasticity, and large deformations. All models were subjected to torsional, two-point loads, and cyclic load using HSC and UHPC. In flexural analysis, the load was applied as a two-point load in the center of beam. In tensional analysis, the load was applied as moment at the end of cantilever beam to create torsion. In cyclic analysis, displacement was applied instead of load in two lines in the mid of beam.

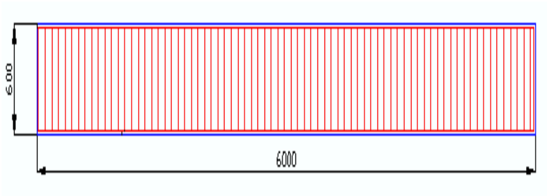

(a) S model: solid beam.

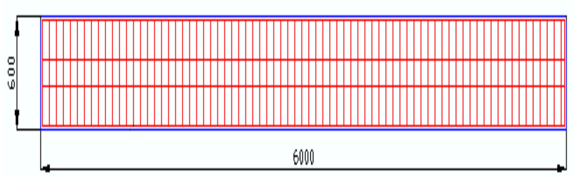

(b) H model: Hollow beam without opening.

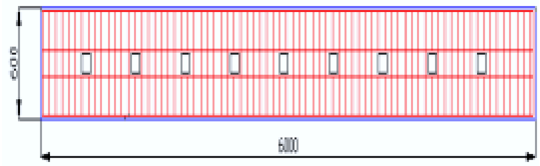

(c) H_{100} model: (100*100) mm opening section, the square opening with depth equal to 16.6% from the depth of the beam.

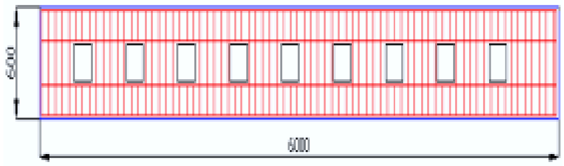

(d) H_{200} model: (200*200) mm opening section, the square opening with depth equal to 33% from the depth of the beam.

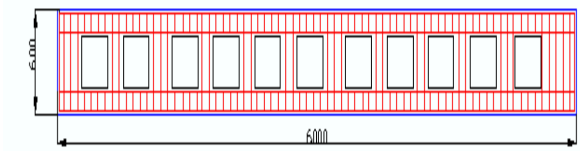

(e) H_{300} model: (300*300) mm opening section, the square opening with depth equal to 50% from the total depth of the beam.

Figure 3: Modeled beams (a) S, (b) H, (c) H_{100}, (d) H_{200}, and (e) H_{300} respectively.

The mechanical properties of concrete and damaged plasticity parameters, as well as the reinforcing bars for all the studied beams, are implemented as the same model for HSC presented by Lopes and Bernardo (2009)and for UHPC reported by Chen and Graybeal (2011).

This study considered the failure criteria in beams during application of load. Concrete damage plasticity for Grade 50 is defined during modeling. All parameters for damaged plasticity are considered based on experimental test reported by Jankowiak and Lodygowski (2005). Model checking failure after analysis is conducted by considering principal stresses and strains and comparing with yield stress in reinforcement and concrete and maximum yield strain. In this study, the yield stress (fy) for reinforcement and concrete are 400 and 50 MPa, respectively. The maximum strain is also considered as 343E-6 for reinforcement.

Notation	Beam type
S	Solid beam
H	Hollow beam
H_{100}	Hollow beam with 100 mm square opening
H_{200}	Hollow beam with 200 mm square opening
H_{300}	Hollow beam with 300 mm square opening

Table 1: Various types of beam considered.

Web opening exists in beam section. Therefore, the model geometry is divided into several parts with simple shapes and less complex geometry to create uniform meshes. To improve the meshing, different mesh algorithms were attempted, and the result with a swept mesh using the medial axis algorithm is shown in Figure 4. All beam models were meshed with 100 mm element.

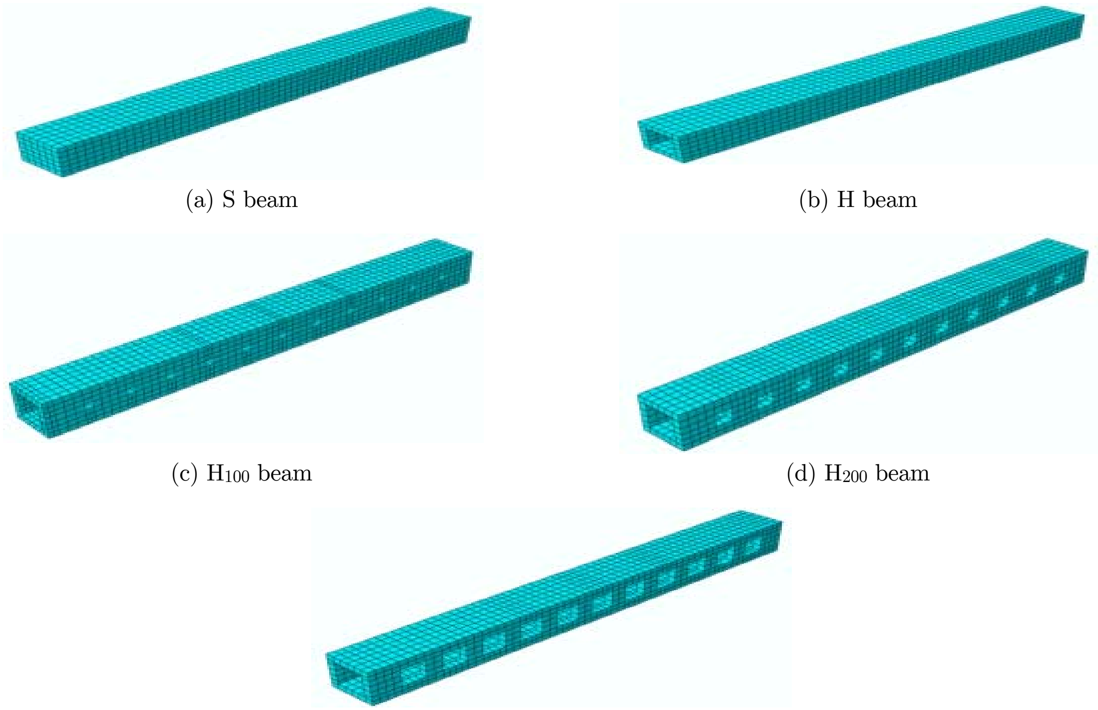

(a) S beam (b) H beam

(c) H_{100} beam (d) H_{200} beam

(e) H300 beam

Figure 4: Meshing for beams (a) S, (b) H, (c) H_{100}, (d) H_{200}, and (e) H_{300}.

The von Mises or Tresca yield criteria are implemented in modeling. In common stress cases, the Von Mises gauge is preferred in cyclic plasticity models because the Tresca yield surface has acute corners in which external normal directions are not evidently defined, and additional parameters must be added to determine the direction of plastic flux at the corners. After the modeling was completed, all beams were subjected to torsional, flexural, and cyclic loads, and results of the analysis were investigated.

3 RESULTS AND DISCUSSION

3.1 Beams Subjected to Torsional Load

All beams were modeled as cantilever beams and subjected to torsional loadings of 400 KN.m for HSC and 700 KN.m for UHPC at the end of the beam to evaluate the effect of torsional load. Therefore, the boundary condition for beam is considered as fix support in one edge and free for the other edge, as shown in Figure 5. Nonlinear analysis was conducted for hollow beams with different opening sizes under torsional load with 0.1 to 0.001 incremental load steps.

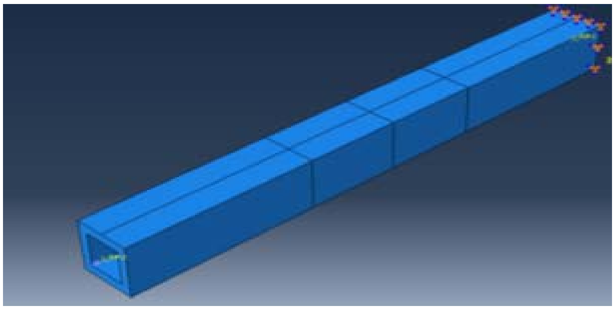

(a) H beam

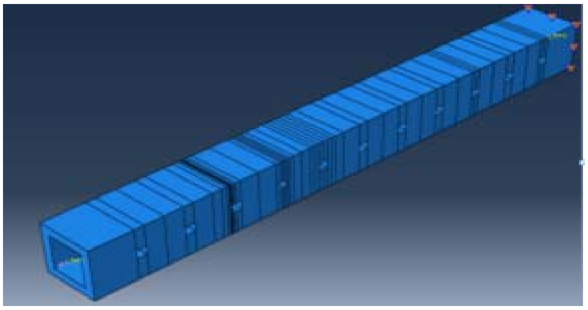

(b) H_{100} beam

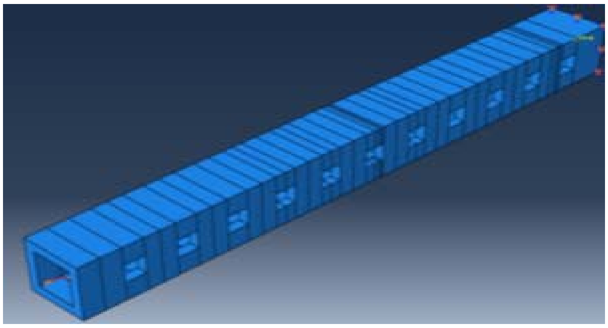

(c) H_{200} beam

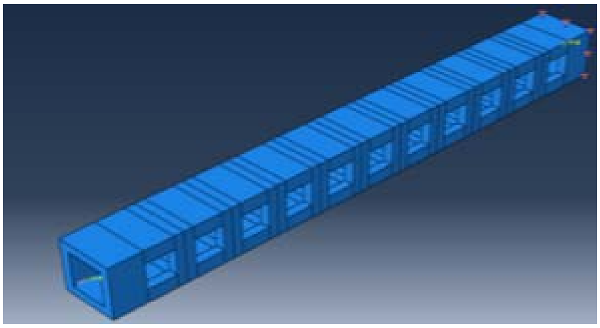

(d) H_{300} beam

Figure 5: Boundary condition and load for beams (a) H, (b) H_{100}, (c) H_{200}, and (d) H_{300} respectively.

The load rotation graphs for HSC and UHPC beams are presented in Figures 6 and 7, respectively. The graph in Figure 6 shows that the capacity of HSC hollow beams with an opening web section was sharply decreased. However, the flexibility in these beams was increased, allowing for increased resistance to more rotation. As shown in Figure 7, the UHPC beam with a square opening depth of 16.6% from the depth of beam H_{100} exhibited a similar response to the hollow beam (H), but the capacity was decreased in beams H_{200} and H_{300}. The results also indicate that the UHPC material led to enhanced capacity of the beam, allowing it to resist twisting, compared with the HSC material.

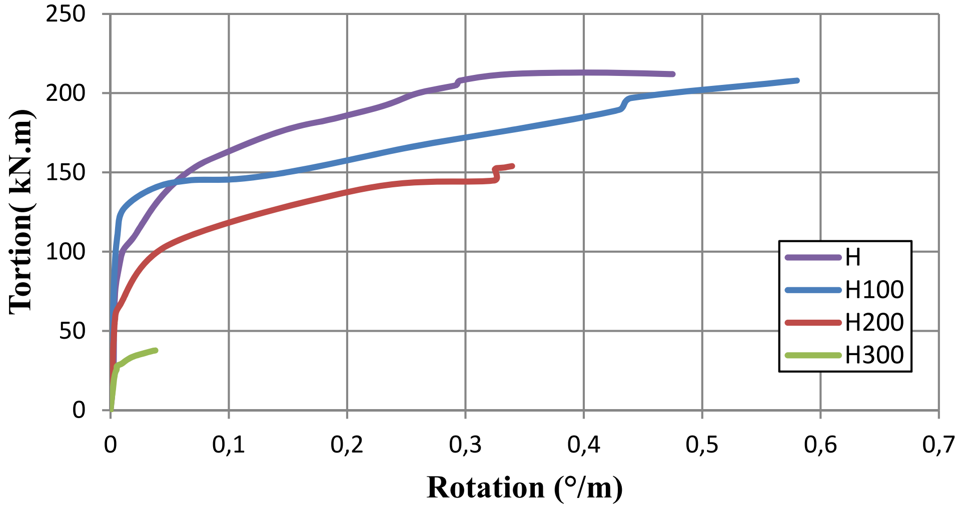

Figure 6: Torsion–rotation curve in beams with HSC.

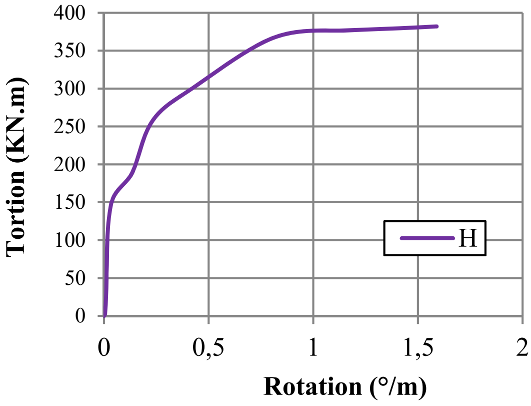

(a) H beam

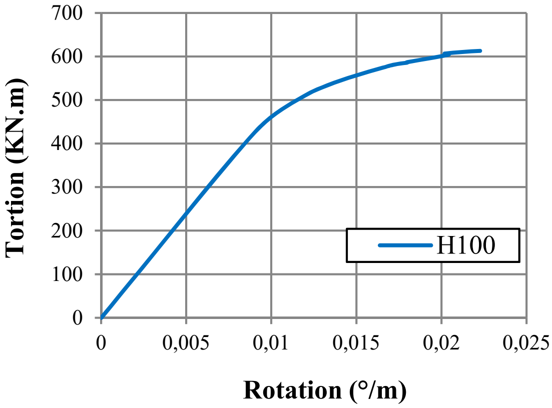

(b) H100 Beam

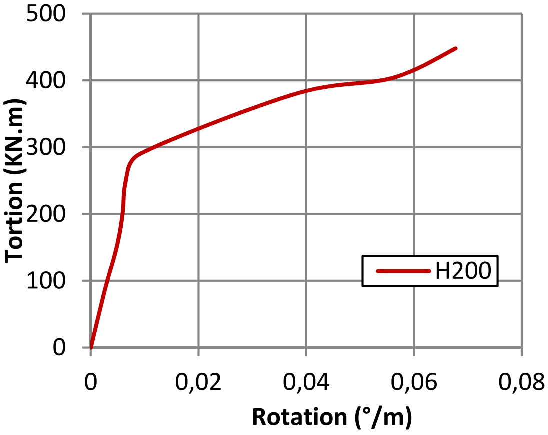

(c) H200 Beam

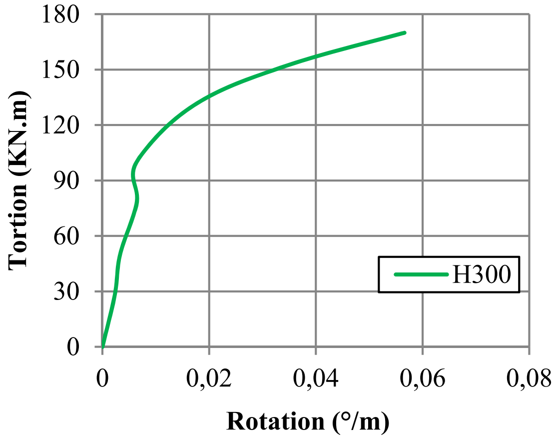

(d) H300 Beam

Figure 7: Torsion–rotation curve in beams with UHPC.

The ultimate torque capacities of the beams are listed in Table 2. The strength of beam (H) was greater than that of beam H100 under pure torsion of about 1.8% for the HSC beam and 12% for the UHPC beam. The ultimate strength in beam H200 was also decreased to 32% for the HSC beam and 35% for the UHPC beam compared with those of beam (H). Similarly, the opening of beam H300 reduced the ultimate strength by about 82% and 75% for HSC and UHPC beams respectively. Therefore, a 12% difference is indicated in the ultimate capacity strength of the UHPC hollow beam with a 100 mm opening size compared with that of beam (H) under pure torsion. This difference leads to reductions in materials and weight of the beam. The stress distributions for all studied beams at the failure stage are presented in Figures 8 and 9 for the HSC and UHPC beams, respectively. As shown in Figures 8 and 9, the stress in the beam with an opening was increased, and the stress distribution around the opening was high for HSC and UHPC beams.

Beams	Torsion (KN.m) HSC			Torsion (KN.m) UHPC		
	Maximum Load	Reduction %	Rotation Θ (°/m)	Maximum Load	Reduction (%)	Rotation Θ (°/m)
H	212	-	0.475	697	-	9.95
H_{100}	208	1.8	0.58	613	12	0.0223
H_{200}	144	32	0.339	448	35	0.0677
H_{300}	37.7	82	0.04	170	75	0.0566

Table 2: Maximum capacity of HSC and UHPC beams under torsion.

The maximum principal stress values in all modeled beams are listed in Table 3. The amount of stress was increased to 94%, 48%, and 45% for beams H_{100}, H_{200}, and H_{300}, respectively, compared with those of the H beam; however, the capacity of $H1_{00}$ was more than that of H_{200} and H_{300}. In addition, the openings in the web section of the UHPC beams led to increases in principal stress, that is, 55% for H_{100}, 93% for H_{200}, and 122% for H_{300}, compared with those of the H beam.

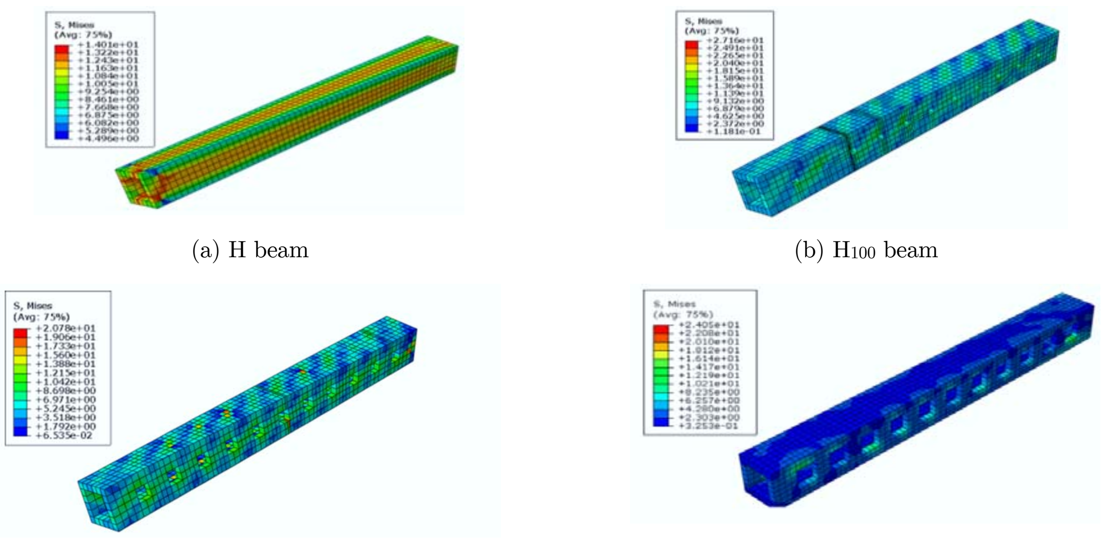

(a) H beam (b) H_{100} beam

(c) H_{200} beam (d) H_{300} beam

Figure 8: Stress distribution for HSC beams.

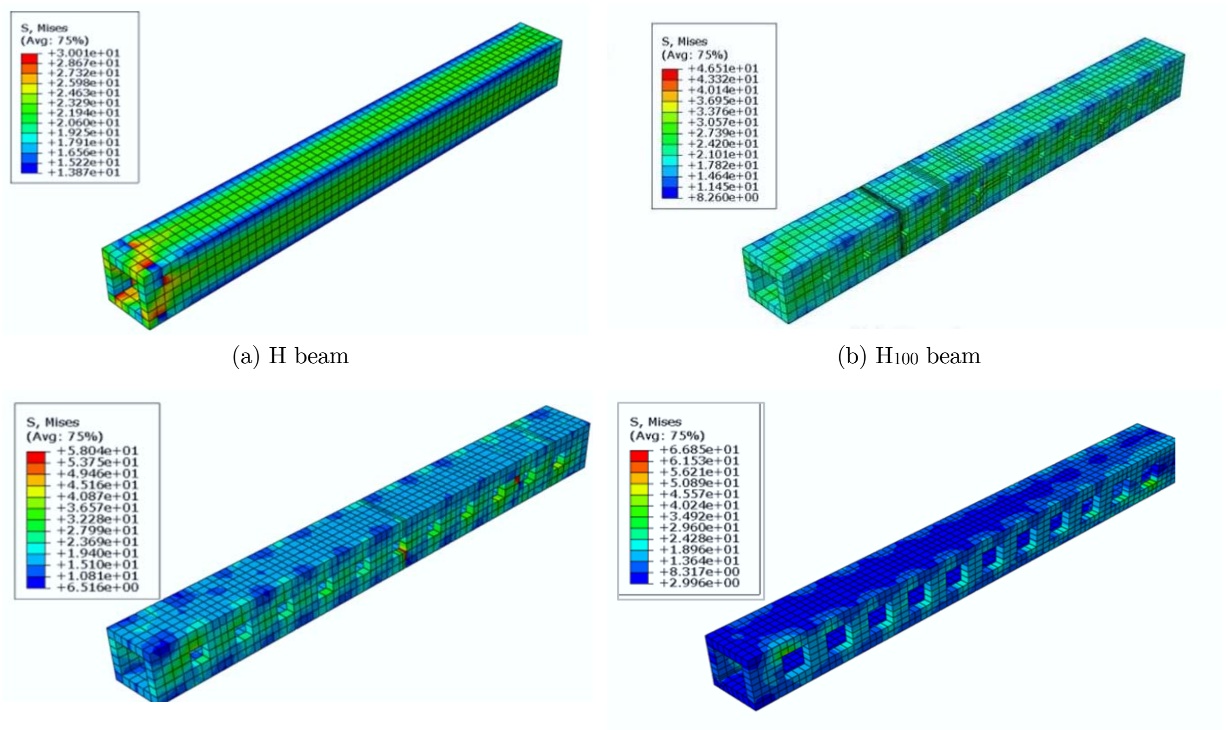

(a) H beam

(b) H_{100} beam

(c) H_{200} beam

(d) H_{300} beam

Figure 9: Stress distribution for UHPC beams.

Beams	HSC		UHPC	
	Stress (MPa)	Increasing %	Stress (MPa)	Reduction %
H	14.01	-	30.10	-
H_{100}	27.16	94	46.51	55
H_{200}	20.87	48	58.04	93
H_{300}	24.50	75	66.85	22

Table 3: Stress distribution for HSC and UHPC beams.

Figures 10 and 11 present the plotted strain distributions of all considered beams. Similar to stress, the maximum strain occurred in the opening area of the beam; however, in the beam (H) without an opening, the maximum strain occurred near the beam support.

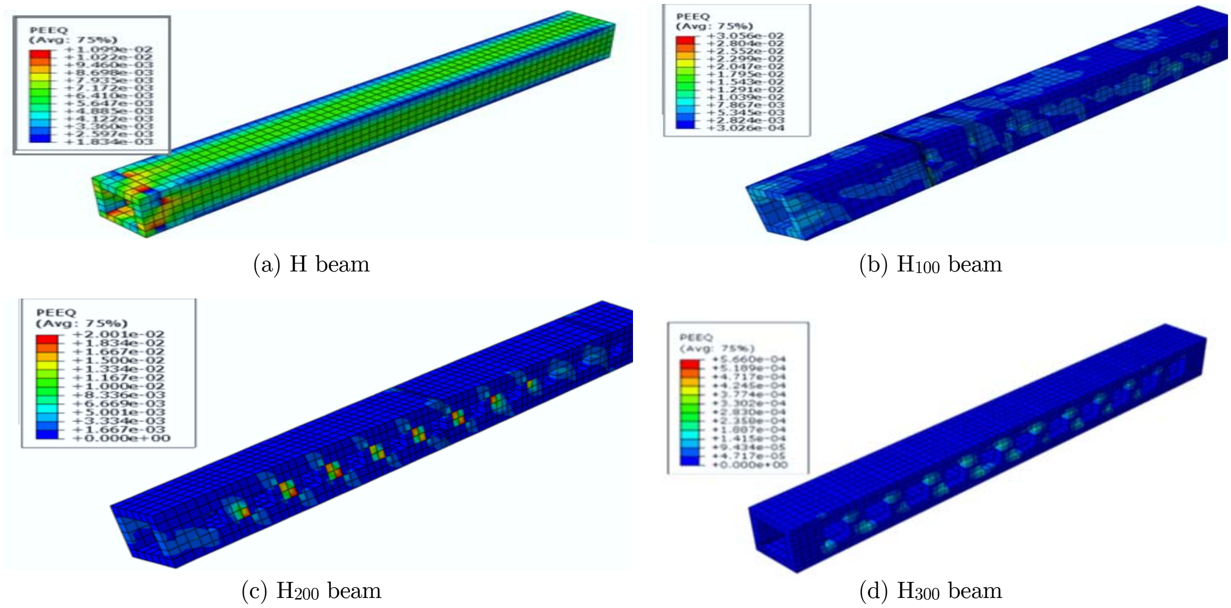

(a) H beam (b) H_{100} beam

(c) H_{200} beam (d) H_{300} beam

Figure 10: Strain distribution for HSC beams.

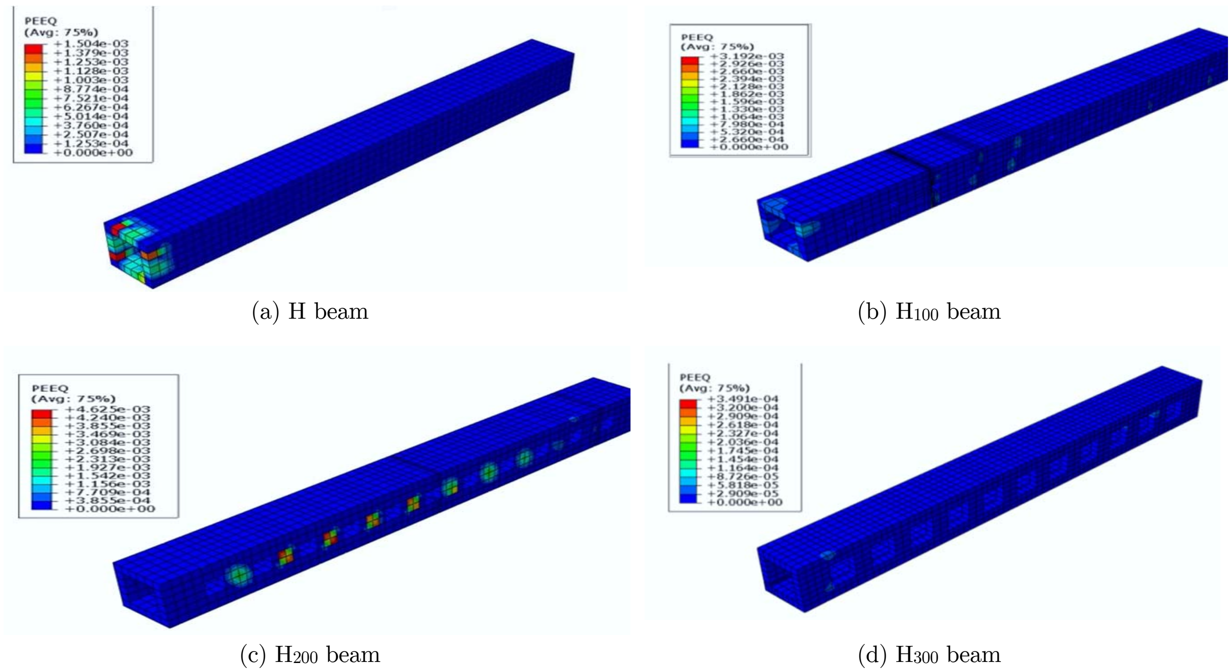

(a) H beam (b) H_{100} beam

(c) H_{200} beam (d) H_{300} beam

Figure 11: Strain distribution for UHPC beams.

The maximum amounts of strain in different beams are presented in Table 4. The opening in the beams led to a considerable increase in maximum strain ranging from 82% to 206% in different HSC and UHPC beams. For the HSC beam (H_{300}), strain was decreased because of reduced load capacity and beam deformation.

Beams	HSC		UHPC	
	Strain (MPa)	Increasing (%)	Strain (MPa)	Increasing (%)
H	0.011	-	0.0015	-
H_{100}	0.031	182	0.0032	113
H_{200}	0.020	82	0.0046	206
H_{300}	0.0006	94	0.0035	133

Table 4: Maximum strain for HSC and UHPC beams under torsional load.

In most design codes of reinforce concrete structures, no specific provision exists for minimum reinforcement amount to ensure a ductile behavior of beams under torsion. The absence of the provision is due to the lack of study on high HSC and UHPFC beams subjected to torsion. Although the minimum amount for reinforcement is mentioned in ACI 318R-05, but an incongruent result may be produced. In MC 90 EC 2 and CSA A23.3-04, the minimum amount of reinforcement is also emphasized.

3.2 Beams Subjected to Flexural Load

This study evaluates the effect of opening on the behavior of hollow beams under flexural load. As shown in Figure 12, all models are loaded symmetrically by two-point loads with a distance of 1000 mm from the center of the beam.

The loads applied on the beams were equal to 300 KN for the HSC and 600 KN for the UHPC because the strength of the UHPC was higher than that of the HSC. The boundary conditions for the simply supported beam at both ends are indicated in Figure 12.

The load deflection of the beams is plotted in Figure 13 for the HSC beams under flexural load. The ductility of the hollow beams was sharply decreased with an increase in the opening size. All hollow beams failed in very small displacements compared with solid beams. All values for the ultimate capacity and maximum deflection of the models are presented in Table 5. The ultimate loads for the solid (S) and hollow beams (H) were 298 and 224 KN, respectively. A marked difference was indicated between the load–deflection curves. A slight difference was observed between the load–deflection curve in beam H_{100} compared with that in the hollow beam. Inserting the square opening with an area equal to 2.2% of the beam web area exerted no effect on the behavior of the beam nor a reduction in ultimate capacity.

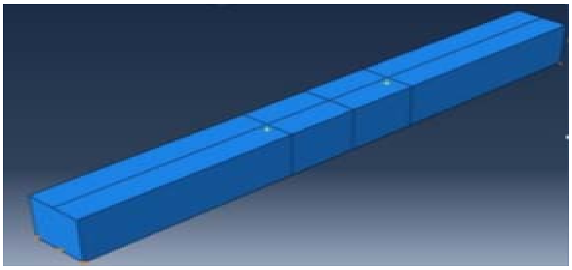

(a) S beam

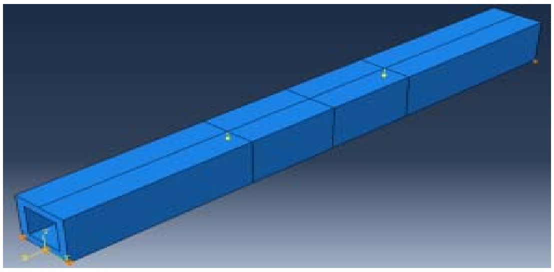

(b) H beam

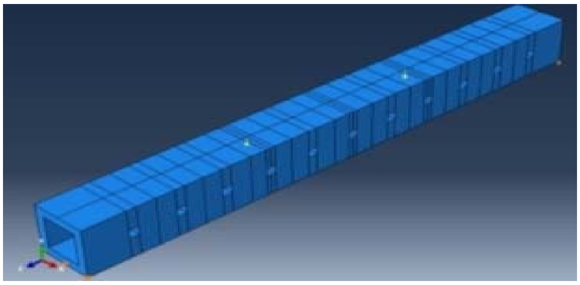

(c) H100 beam

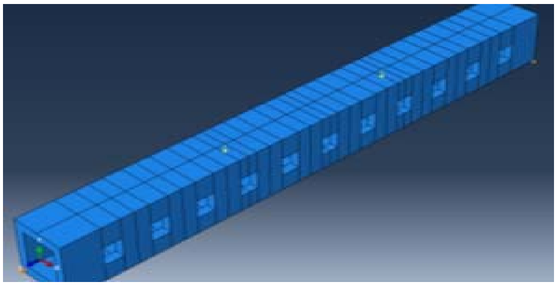

(d) H200 beam

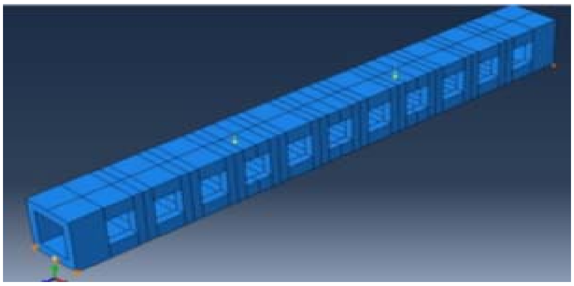

(e) H300 beam

Figure 12: Flexural load applied on beams.

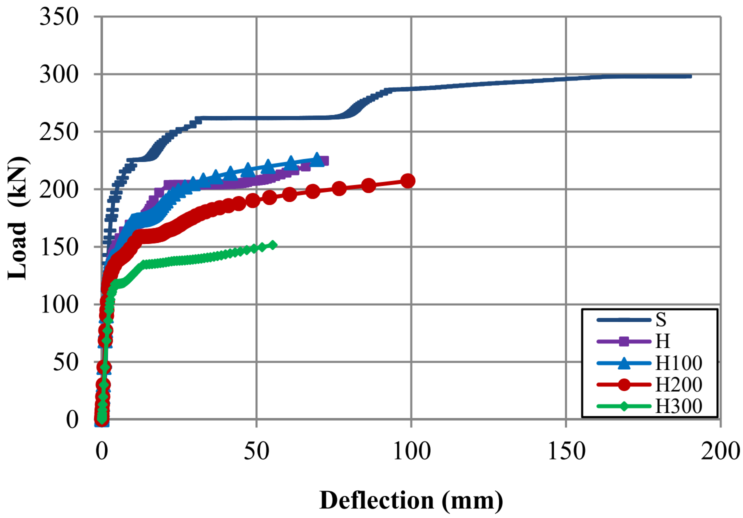

Figure 13: Load–deflection curve for HSC.

Beams	Load		Area under curve		Displacement (mm)		ductility
	Ultimate load (KN)	Reduction (%)	Capacity	Reduction (%)	At maximum force	At 0.85 from maximum load	
S	298	-	51,570,010	-	188.6	23	8.2
H	224	24.8	14,022,103	72.8	71.8	17	4.2
H_{100}	226	24.2	13685004	73.4	69.5	22	3.2
H_{200}	207	30.5	17948237	65.1	68.2	29	2.4
H_{300}	152	49	7390144	85.6	55.2	15	3.6

Table 5: Ultimate load for HSC beams under flexural load.

The ultimate load capacities for the beam models H_{200} and H_{300} were reduced to 207 and 152 KN, respectively. Therefore, using the hollow beam and beam H_{100} led to a decrease of up to 24% in ultimate load. In models H_{200} and H_{300}, the reductions in ultimate load were up to 30% and 49%, respectively, for the HSC. Therefore, openings in hollow beams effectively reduced the load capacity of beams during flexural loading. The beam with a square opening depth equal to 16.6% from the depth of beam H_{100} responded almost similarly with the hollow beam without an opening (H). Meanwhile, load capacity was decreased in beams H_{200} and H_{300}.

The area under the load–deflection curve was reduced by 72.8% for the hollow beam compared with the solid beam; it was also reduced by about 73.2%, 65.1%, and 85.6% for beams H_{100}, H_{200}, and H_{300}, respectively. This result indicates that the beam opening partially reduced the flexibility of the beam.

The ductility of the hollow beam was 4.2, which is half of that of the solid beam (8.2) and was reduced slightly for the hollow beams with openings (H_{100}, H_{200}, and H_{300}).

The load deflection results for the UHPC beams subjected to a couple concentrated load of 600 KN are depicted in Figure 14. As shown in the graph, the strength and flexibility of hollow beams with openings were markedly reduced and the beams exhibited brittleness.

Based on the results presented in Table 6, the ultimate loads for the S and H beams were 1322 and 767 KN, respectively, indicating a 42% reduction in ultimate load.

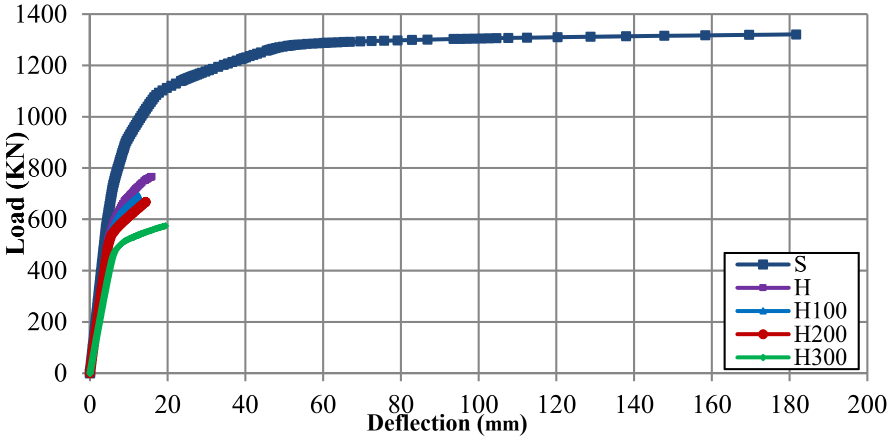

Figure 14: Load–deflection curve for UHPC.

Beam	Load (KN)	Percentage (%)	Area under curve	Reduction percentage (%)	Displacement (mm)		Ductility
					At maxi-mumforce	At 0.85 from-maximum load	
S	1322	-	52,137,256	-	182	19	9.5
H	767	42	1,396,684	97	16	8	2
H_{100}	692	48	925,356	98	12	6.5	1.8
H_{200}	668	49	1,093,524	98	14	7.1	1.9
H_{300}	575	56	1,533,305	97	19	8	2.4

Table 6: UHPC beams under flexural load.

The hollow beams with various opening sizes (H_{100}, H_{200}, and H_{300}) were reduced almost similarly in the range of 48% to 56%, and the ultimate strengths were reduced to 692, 668, and 575 KN, respectively. Such reductions were attributed to severe bending of the material from the compression zone, thereby minimizing the concrete area required for the expansion of the total compressive stress block at the ultimate load.

In addition, the displacement and the area under the curve in all hollow section beams showed almost similar reduction of 10 times compared with the solid beam S, which is affected by beam ductility. The ductility of the solid beams was 9.5, whereas all other hollow beams (H_{100}, H_{200}, and H_{300}) exhibited almost the same degree of ductility.

Comparison of the results for HSC and UHPC in Table 7 shows that the hollow section and the openings in the beam web strongly affected the ultimate load in the UHPC beams than in the HSC beams. Using UHPC instead of HSC allowed the beams to carry more load ranging from 67% to 77% by reducing the number of reinforcement for the same beams under a point load.

The effect of the hollow section with an opening in the area under curve was about 97% reduction; the reduction in HSC ranged from 65% to 85% only, indicating a smaller effect, compared with that in the UHPC beams.

Beam	Ultimate load (KN)			Area under curve		
	HSC	UHPC	Comparison of ultimilate load between HSC and UHPC (%)	HSC	UHPC	Comparison of area under curve between HSC and UHPC (%)
S	298	1322	0.77	51,570,010	52,137,256	-1.09
H	225	767	0.71	14,022,103	1,396,684	90
H_{100}	226	692	0.67	1,3685,004	925,356	93
H_{200}	207	668	0.69	17,948,237	1,093,524	94
H_{300}	152	575	0.74	7390144	1,533,305	79

Table 7: UHPC and HSC under flexural load.

3.3 Beams Subjected to Cyclic Loading

To evaluate the effect of a hollow section with an opening on a beam subjected to dynamic loading, all considered models were subjected to cyclic displacement. The amplitude of displacement applied was 100 mm for the HSC beam and 200 mm for the UHPC beam; the history of displacement is presented in Figure 15(a). The boundary conditions were applied to the support nodes as roller and pinned supports in another end of the beam, as shown in Figure 15(b).

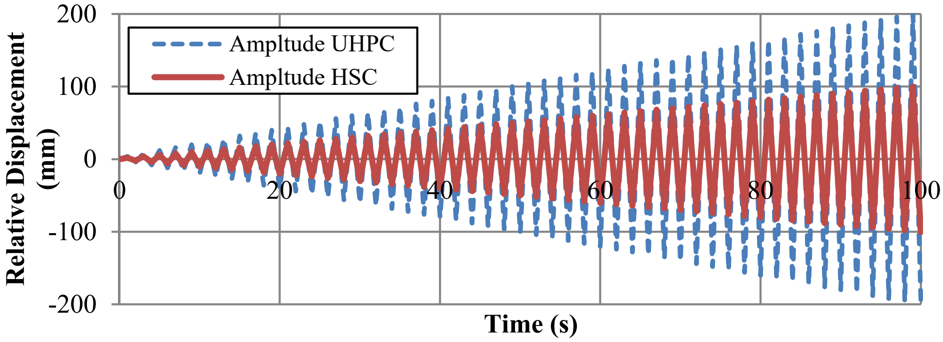

Figure 15: (a) Relative displacement vs time.

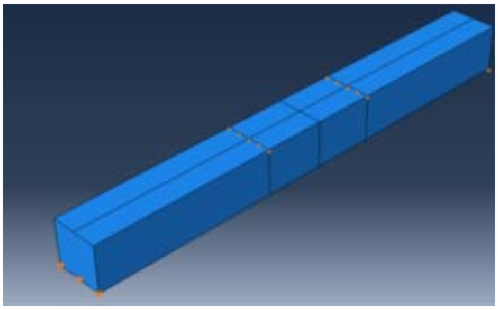

S beam

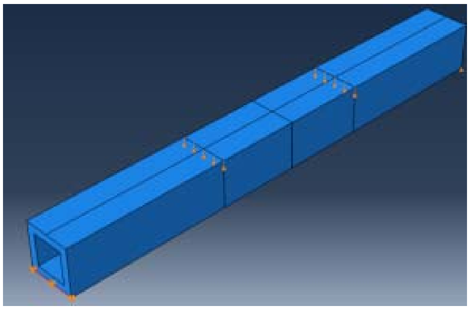

H beam

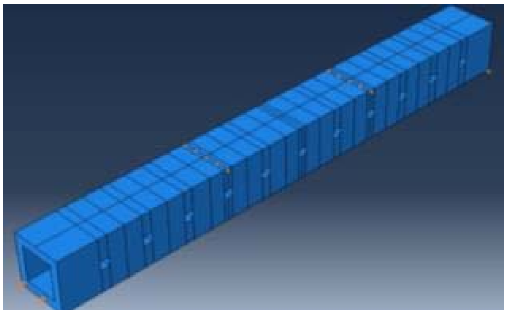

H100 beam

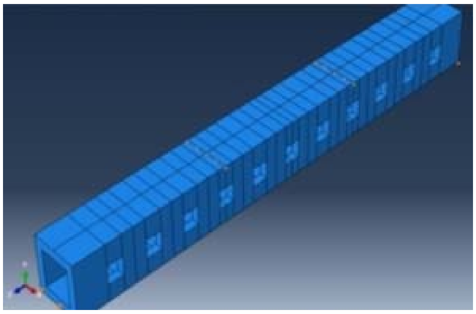

H200 beam

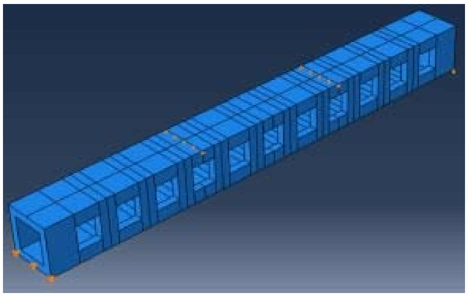

H300 beam

Figure 15: (b) Cyclic load applied on beams.

The hysteresis analysis for the cyclic loading of the HSC and UHPC beams is presented in Figures 16 and 17. A marked difference is indicated between the load–deflection curves of the hollow beams compared with the solid beam. In addition, the capacity of the hollow beams (H_{100}, H_{200}, H_{300}) was reduced with the increase of the size of the opening section.

The results listed in Table 8 indicate that the ultimate loads for the solid (S) and hollow (H) beams were 349 and 213 KN, respectively. Therefore, the use of the H beam reduced the ultimate load by 38%. The beam H_{100} also showed a similar reduction. The maximum loads for H_{100}, H_{200} and H_{300} were about 216, 163, and 96 KN, respectively, presenting gradual reductions in the ultimate load capacity of about 53% and 73%, compared with those of the solid beam.

The energy dissipation for all hollow sections beams was substantially reduced from 86% to 95%, indicating a noticeable deduction in beam performance. Meanwhile, the ductility index for the solid beam was 4.2, which is largely reduced to 1.3 in the hollow beam without an opening (H).

The ductility index was increased in beams H_{100} and H_{200} to 6.9 and 5.4, respectively; however, by increasing the opening size of beam H_{300}, ductility was further reduced to 3.4.

Figure 17 presents the hysteresis plot of all considered UHPC beams. Similar to the HSC beams, the performance of the hollow beams decreased.

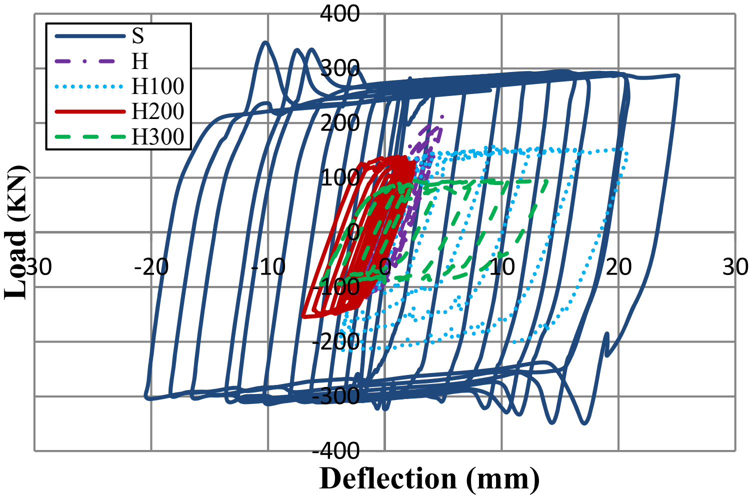

Figure 16: Load–deflection HSC hysteresis loop.

Beam	Load (KN)	Reduction (%)	Energy dissipation		Displacement		Ductility
			Area	Increasing (%)	At maximumforce (mm)	At 0.85 frommaximum load	
S	349	-	1.35E+08	-	25	6	4.2
H	213	39	10842493	92	5	3.9	1.3
H_{100}	216	38	18405675	86	20.8	3	6.9
H_{200}	163	53	11427616	91	97.6	18	5.4
H_{300}	96	73	6937206	95	13.8	4	3.4

Table 8: HSC beams under cyclic load.

The hysteresis graph representing the cyclic load of the UHPC beams is plotted in Figure 18, and the analysis is presented in Table 9. The ultimate load for solid beam (S) was about 1234 KN and that for hollow the beam (H) was about 984.3 KN, indicating a 20% reduction in ultimate load. Meanwhile, the maximum load of beams H_{100}, H_{200}, and H_{300} were 733, 718.4, and 564 KN, respectively. The reductions were about 40%, 42%, and 54%, respectively. The result also shows that the reduction in capacity (area under the curve) for the hollow beam (H) was 88%, whereas those for the beams H_{100}, H_{200}, and H_{300} were 98%, 95%, and 97%, indicating high reduction in the capacity of the hollow beams compared with that of the solid beam. The ductility of the solid beam (S) was 3.9, whereas that of the hollow beam was about 2.4, For beams H_{100}, H_{200}, and H_{300}, the values for ductility were 2.3, 1.1, and 1.82, respectively.

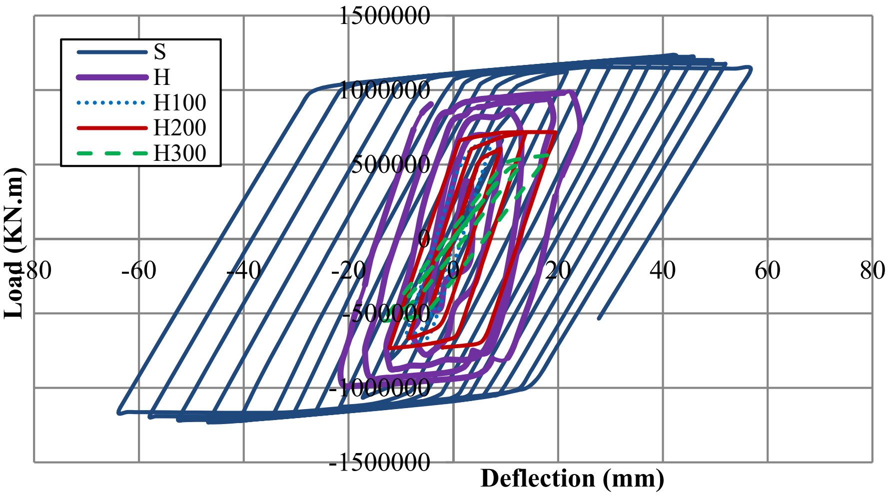

Figure 17: Load–deflection UHPC hysteresis loop.

Beam	Load (KN)	Percentage (%)	Energy dissipation		Displacement		Ductility
			Under curve area	Percentage (%)	At maximum force (mm)	At 0.85 from-maximum load	
S	1234	-	1.4E0+9	-	42.4	11	3.9
H	984.3	20	1.6E0+8	88	21.5	9	2.4
H_{100}	733	40	25373924	98	10.2	4.5	2.3
H_{200}	718.4	42	67169799	95	7.65	7	1.1
H_{300}	564	54	38703591	97	18.2	10	1.82

Table 9: UHPC beams under cyclic displacement load.

Table 10 presents a comparison of the ultimate load capacity resulting from cyclic analysis for HSC and UHPC beams. The results indicate that using UHPC instead of HSC led to a 70% increase in carrying load, which reveals an economical design.

Beam	Cyclic load		Reduction percentage (%)
	HSC	UHPC	
S	349	1234	0.72
H	213	984.3	0.78
H_{100}	216	733	0.67
H_{200}	163	718.4	0.77
H_{300}	96	564	0.71

Table 10: Comparison of ultimate load capacity between UHPC and HSC beams under cyclic load.

This study mainly evaluated the effect of an opening on beam under similar conditions of geometry and material, as well as reinforcement arrangement, to elucidate the reduction of strength and flexibility of beams caused by opening in web section. This issue can be rectified by adding more reinforcement or using high concrete grade, but it is not feasible in some cases because of consternation criteria, such as limitation in space and simplification of construction process.

4 CONCLUSIONS

In this paper, the effects of varying sizes of square openings in the web of hollow beams on the behavior of the beams subjected to different types of loading were investigated and compared with those of the solid beam. High-strength concrete and ultra-high performance concrete were employed. For this purpose, the hollow beam with openings of different sizes was modeled using the finite element method. Nonlinear analysis was conducted for developed models under torsional, flexural, and cyclic loads.

The torsional load showed that the strength of the hollow beam (H) was greater than that of beam H_{100} under pure torsion of about 1.8% for the HSC beam and 12% for the UHPC beam. Compared with that of the hollow beam (H), the ultimate strengths in beams H_{200} and H_{300} were decreased to approximately 32% to 82% for the HSC beam and 35% to 75% for the UHPC beam, respectively. In addition, the results for stress and strain in the hollow beam with an opening were markedly increased compared with those of the hollow beams without an opening; the stress distribution was wider around the opening in the web of beam for both HSC and UHPC materials.

The results of flexural load on the beams indicated 24% and 42% reductions in ultimate loads for the HSC and UHPC, respectively, compared with those of the solid beam. The opening in the hollow beams effectively reduced the capacity of beams for flexural loading. The beam with a square opening depth equal to 16.6% from the depth of the beam (H_{100}) responded almost similarly with the hollow beam without an opening (H). Meanwhile, the capacity was decreased in beams H_{200} and H_{300}.

The reductions in displacement and load bearing in all hollow section beams were almost similar and about 10 and 3 times that for the HSC and UHPC beams, respectively, compared with the solid beam (S), leading to a large reduction in ductility.

The results for the beam subjected to cyclic loads indicate that the ultimate load of the hollow beam (H) compared with that of the solid beam was reduced by about 39% for the HSC and 20% for the UHPC. The reduction was about 38% for both H and H_{100} beams for HSC, whereas the reduction was about 20% and 40% for H and H_{100} beams, respectively, for UHPC. Therefore, energy dissipation in both types of beams were highly reduced by about 86% to 98% for the hollow beams with and without an opening, indicating minimized performance of beam subjected to dynamic loads.

References

Bernardo, L., and Lopes, S. (2013). Plastic analysis and twist capacity of high-strength concrete hollow beams under pure torsion. Engineering Structures, 49, 190-201.

Chen, L., and Graybeal, B. A. (2011). Modeling structural performance of ultrahigh performance concrete I-girders. Journal of Bridge Engineering.

Guleria, A. (2014). Comparison of Seismic Performance of Solid and Hollow Reinforced Concrete members in RCC framed Building using ETABS Software. International Journal of Advances in Engineering Sciences, 4(4), 43-47.

Hafiz, R. B., Ahmed, S., Barua, S., and Chowdhury, S. R. (2014). Effects of Opening on the Behavior of Reinforced Concrete Beam.

Hii, A. K., and Al-Mahaidi, R. (2006). An experimental and numerical investigation on torsional strengthening of solid and box-section RC beams using CFRP laminates. Composite structures, 75(1), 213-221.

Inoue, S., and Egawa, N. (1996). Flexural and Shear Behavior of Reinforced Concrete Hollow Beams under Reversed Cyclic Loads. Paper presented at the Proceedings of 11th World Conference on Earthquake Engineering. Paper.

Jankowiak, T., and Lodygowski, T. (2005). Identification of parameters of concrete damage plasticity constitutive model. Foundations of civil and environmental engineering, 6(1), 53-69.

Li, B., Reis, L., and De Freitas, M. (2006). Simulation of cyclic stress/strain evolutions for multiaxial fatigue life prediction. International Journal of Fatigue, 28(5), 451-458.

Lopes, S., and Bernardo, L. (2009). Twist behavior of high-strength concrete hollow beams–formation of plastic hinges along the length. Engineering Structures, 31(1), 138-149.

Lopes, S., and Bernardo, L. (2014). Cracking and failure mode in HSC hollow beams under torsion. Construction and Building Materials, 51, 163-178.

Mohamed, A. R., Shoukry, M. S., and Saeed, J. M. (2014). Prediction of the behavior of reinforced concrete deep beams with web openings using the finite element method. Alexandria Engineering Journal, 53(2), 329-339.

Namiq, Z. F. (2008). ⊠Design Of Beam As A Hollow Cross Section By Using Steel Fiber Under Pure Torsion ⊠. M. Sc. thesis, University of Salahaddin, Hawler Iraq.

Patel, K., BHARDWAJ, A., CHAUDHARY, S., and Nagpal, A. (2014). Explicit expression for effective moment of inertia of RC beams. Latin American Journal of Solids and Structures, an ABCM Journal, 12(3), 542-560.

Torii, A. J., and Machado, R. D. (2012). Structural dynamic analysis for time response of bars and trusses using the generalized finite element method. Latin American Journal of Solids and Structures, 9(3), 1-31.

Yoo, D.-Y., and Yoon, Y.-S. (2015). Structural performance of ultra-high-performance concrete beams with different steel fibers. Engineering Structures, 102, 409-423.